Article

pubs.acs.org/Biomac

Influence of Polyelectrolyte Film Stiffness on Bacterial Growth

Naresh Saha,[†,‡] Claire Monge,[‡] Virginie Dulong,[§] Catherine Picart,[‡] and Karine Glinel*[,†]

[†]Institute of Condensed Matter and Nanosciences, Bio- & Soft Matter Division, Université catholique de Louvain, Croix du Sud 1, 1348 Louvain-la-Neuve, Belgium

[‡]LMGP, CNRS UMR 5628, Grenoble Institute of Technology, 3 parvis L. Néel, F-38016 Grenoble cedex, France

[§]Laboratoire Polymères, Biopolymères, Surfaces, CNRS UMR 6270, Université de Rouen, Bd Maurice de Broglie, F-76821 Mont Saint Aignan, France

Supporting Information

ABSTRACT: Photo-cross-linkable polyelectrolyte films, whose nanomechanical properties can be varied under UV light illumination, were prepared from poly(L-lysine) (PLL) and a hyaluronan derivative modified with photoreactive vinylbenzyl groups (HAVB). The adhesion and the growth of two model bacteria, namely *Escherichia coli* and *Lactococcus lactis*, were studied on non-cross-linked and cross-linked films to investigate how the film stiffness influences the bacterial behavior. While the Gram positive *L. lactis* was shown to grow slowly on both films, independently of their rigidity, the Gram negative *E. coli* exhibited a more rapid growth on non-cross-linked softer films compared to the stiffer ones. Experiments performed on photopatterned films showing both soft and stiff regions, confirmed a faster development of *E. coli* colonies on softer regions. Interestingly, this behavior is opposite to the one reported before for mammalian cells. Therefore, the photo-cross-linked (PLL/HAVB) films are interesting coatings for tissue engineering since they promote the growth of mammalian cells while limiting the bacterial colonization.

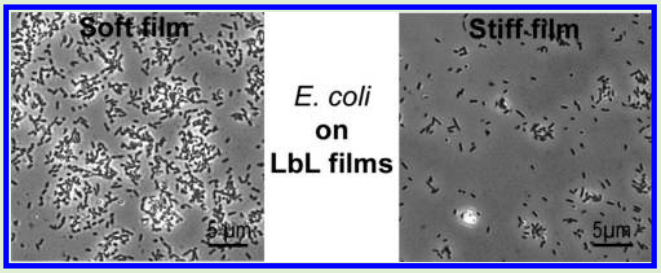

INTRODUCTION

Bacterial adhesion and biofilm development on medical devices represent a pending problem which causes a large part of hospital-acquired infections.[1−4] Notably, biomaterial-associated infections are considered to be a major cause of implant failure. The proper integration of a medical implant depends on the competition between host tissue integration and bacterial colonization.[5,6] Therefore, the development of material surfaces, which promote the proliferation of eukaryotic cells in a controlled way while decreasing the development of biofilms remains a major challenge. Current approaches to limit bacterial development on biomaterial surfaces are based on the immobilization of bactericidal agents such as antibiotics or silver nanoparticles.[7−11] However, a major concern about these strategies is the potential cytoxicity of the antimicrobial agents or their role in the emergence of multiresisting pathogens.[12−14]

Although physicochemical properties of the surface are known to affect the bacterial adhesion and proliferation,[15] they were poorly explored to reduce or to slow down the colonization of biomaterial surfaces. Charge and hydrophobicity of the surface have been reported to play an important role during the primary step of bacterial adhesion.[16−18] Moreover, very recent studies performed on nanostructured surfaces showed that the nanostructure affects bacterial adhesion and biofilm formation and more importantly individual bacterial cell function.[19−24]

By contrast, it is now well established that physicochemical properties of the surface such as chemistry, topography, and mechanical properties modulate the adhesion and the response of eukaryotic cells.[25−29] Notably, it was shown that the mechanical stiffness of the substrate impacts significantly the adhesion and the proliferation of mammalian cells and more interestingly their function.[30−33] However this parameter has been barely explored as far as bacterial adhesion is concerned.[34−36] Van der Mei et al. reported notably that marine bacteria adhered in higher numbers on polyurethane (PU) substrates of higher cross-linking density and therefore higher rigidity, under certain flow chamber conditions.[36]

The layer-by-layer (LbL) deposition of polyelectrolytes onto solid substrates is a versatile and easy-to-perform technique to produce thin films with various surface properties depending on the nature of polyelectrolytes used and the post-treatments performed.[37,38] Moreover, the LbL technique can be applied to a wide range of substrata such as glasses, metals, or plastics. During the last decades, numerous studies have focused on the development of biofunctional LbL films promoting mammalian cell adhesion for tissue engineering applications.[39,40] It was notably shown that chemically cross-linked LbL films based on biopolymers promote the adhesion of various mammalian cells

Received: November 14, 2012
Revised: January 4, 2013
Published: January 6, 2013

due to their higher elastic modulus.[41] Van Vliet et al. reported the preparation of LbL films based on weak synthetic polyelectrolytes whose mechanical stiffness can be varied by changing the pH of the dipping solutions of polyanion and polycation.[34] Bacterial assays performed on these films suggested that an increase of the film stiffness promoted cell adhesion and colony growth. Recently, we have elaborated polyelectrolyte films based on biopolymers and whose mechanical properties can be reinforced through a UV light exposure.[42] To this end, an anionic hyaluronic acid derivative grafted with vinylbenzyl groups (HAVB) was LbL assembled with cationic poly(L-lysine) (PLL) onto a solid substrate (Scheme 1). The resulting multilayers were subsequently

Scheme 1. Preparation of Photo-Cross-Linked (PLL/HAVB) LbL Films

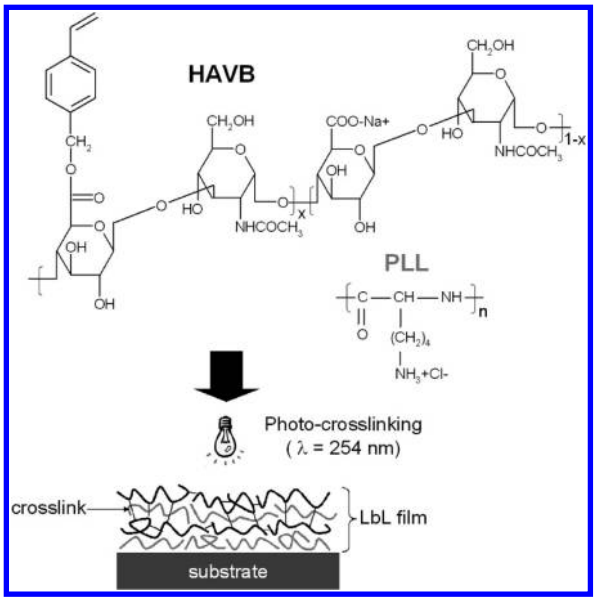

photo-cross-linked under UV light to increase their stiffness. By varying the content of VB groups grafted on the HA derivative and the exposure time, we showed that the elastic modulus of the films varied from 30 to 150 kPa.[42] The photo-cross-linking results in the formation of a C−C bond between vinyl groups present on HAVB chains. This methodology allowed us to vary the film mechanical properties without significantly changing their charge density, surface chemistry, and morphology in contrast with other processes based on chemical cross-linking or pH variations. Moreover, the photo-cross-linking is a clean and mild process avoiding the addition of potentially toxic substances. The adhesion and proliferation of C2C12 myoblasts on these films was shown to increase with the cross-linking degree.[42]

Here, we propose to test the adhesion of bacteria on these films and to investigate the influence of the film stiffness on the bacterial response. The idea is to explore whether the film stiffness is a relevant physicochemical parameter to discriminate the adhesion and growth of mammalian and bacterial cells onto solid substrates. We thus paid special attention to keep constant all chemical and morphological characteristics of the films, while varying only their rigidity, by using the photo-cross-linkable system described in Scheme 1. Two types of well-established model bacteria, namely *Lactococcus lactis* and *Escherichia coli*, which differ by their shape, their Gram-stain class, and their growth conditions, were tested to evaluate whether the bacterial behavior observed on films of varying rigidity was influenced by the bacterial type.

EXPERIMENTAL SECTION

Materials. PLL (70 000 g·mol^{-1}) and hyaluronic acid (HA, 200 000 g·mol^{-1}) were supplied by Sigma-Aldrich (Benelux) and Lifecore Biomedical (USA), respectively. 4-Vinylbenzyl chloride was purchased from Acros (France) and was used without further purification. HA grafted by 37% of 4-vinylbenzyl groups ($HAVB_{37}$) was synthesized as described previously.[42] All the solvents and salts used were of analytical grade. Water was Milli-Q grade (resistivity higher than 18.2 MΩ cm).

Preparation of Polyelectrolyte Films. PLL and $HAVB_{37}$ were dissolved in 0.15 M NaCl at 0.5 and 1 g·L^{-1}, respectively. The pH of the solutions was set at pH 7.4 by adding 0.1 M NaOH. All solutions were filtered through a 8 μm Millipore membrane before use. The substrates used for multilayer growth were circular glass coverslips of 14 mm in diameter or fused silica slides (Hellma, France). They were cleaned by treatment in a hot piranha solution (H_2O_2 (35%)/H_2SO_4 (98%), 1:1, v/v) for 20 min (*caution: piranha solution is extremely corrosive*) and then thoroughly washed with pure Milli-Q water. The films were fabricated manually by alternately dipping the substrate in aqueous solutions of PLL and $HAVB_{37}$ for 10 min each. Between each deposition step, the substrate was thoroughly rinsed with a 0.15 M NaCl solution buffered at pH 7.4 to remove the excess polyelectrolyte. Films used in this study were prepared by 12 deposition cycles of PLL and $HAVB_{37}$ leading to $(PLL/HAVB_{37})_{12}$ films.

Photo-Cross-Linking of Polyelectrolyte Films. Freshly prepared $(PLL/HAVB_{37})_{12}$ films were cross-linked directly in buffer solution by exposure during 40 min at a distance of 12 cm to a model VL-215.LC (Vilber Lourmat) short-wave ultraviolet lamp (30 W) transmitting at 254 nm. The incoming UV intensity measured in these conditions with a VLX-3W radiometer was 0.5 mW cm^{-2}.

Photopatterned films showing a pattern of rigidity were prepared according to the process described in Scheme 2. LbL assembly of PLL and HAVB was performed onto a transparent SUPRASIL-type fused silica substrate incorporating a metal grid playing the role of a photomask. The fabrication of this substrate was described in detail elsewhere.[43] After the deposition of 12 pairs of layers, the photo-cross-linking was performed by immersing the film upside down in buffer solution and exposing it to UV light according to the conditions

Scheme 2. Preparation of Photo-Patterned Films Using a Transparent Substrate Incorporating a Photomask[a]

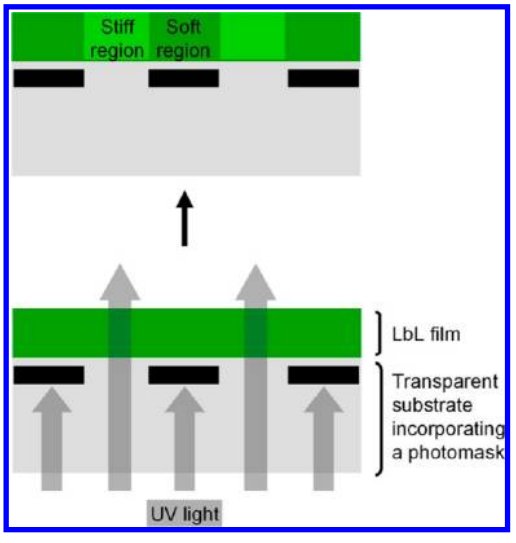

[a]The film, which is deposited on the substrate, is photo-irradiated by UV light.

dx.doi.org/10.1021/bm301774a | *Biomacromolecules* 2013, 14, 520−528

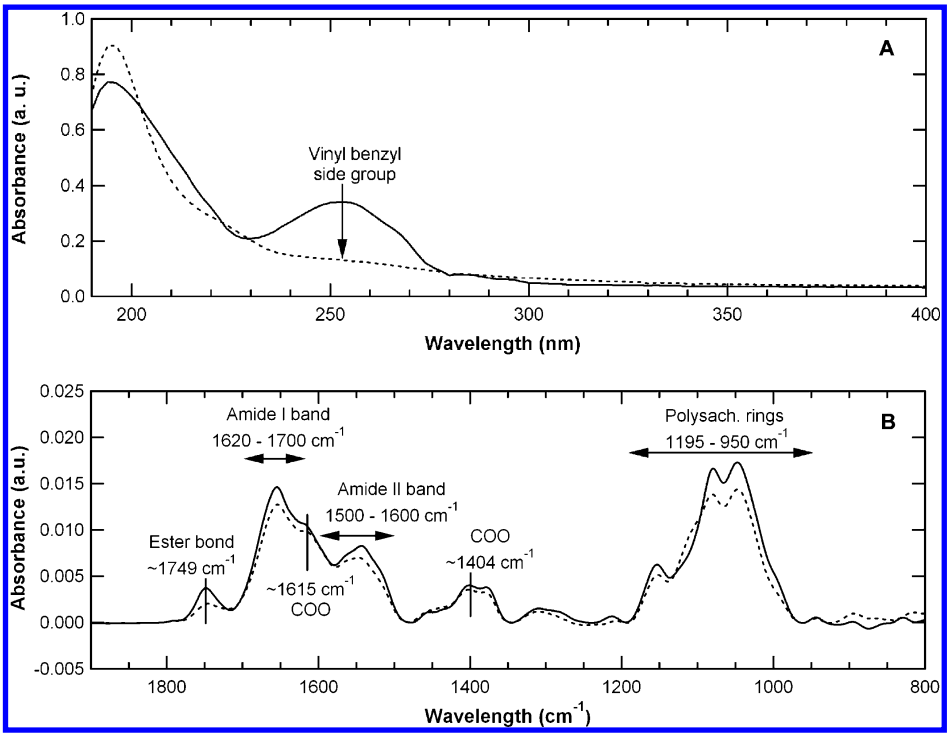

Figure 1. UV−vis spectroscopy (A) and FTIR spectroscopy (B) measurements performed on (PLL/HAVB$_{37}$) films before (continuous line) and after photo-cross-linking (dashed line); the UV exposure time used to achieve photo-cross-linking was 40 min.

described above. This protocol prevented any contact between the photomask and the polyelectrolyte film, thereby preserving its physical integrity.

Film Characterization. (PLL/HAVB$_{37}$)$_{15}$ films deposited onto fused silica slides (Hellma, France) were measured before and after photo-cross-linking with a Kontron UVIKON860 UV−vis spectrometer. The spectra were collected using an uncoated fused silica slide as a reference.

A Vertex 70 spectrophotometer (Bruker Optics Gmbh, Ettlingen, Germany) was used for the acquisition of FTIR spectra. Films built in 0.15 M D_2O on a silicon substrate and subsequently dried were studied in transmission mode. Single-channel spectra were recorded between 400 and 2000 cm^{-1} with a 2 cm^{-1} resolution by means of the OPUS Software v6.5 (Bruker).

Contact angle measurements were performed in the captive air bubble configuration, using a home-built copper cell with glass windows, filled with Milli-Q water. An air bubble of about 1 mm diameter was trapped below the samples, and images of the bubble were taken with a digital camera. The bubble shape was then fit near the triple line by arcs of a circle, using a home-written program, and the left and right contact angles were averaged to obtain the contact angle.

AFM imaging of homogeneous non-cross-linked and photo-cross-linked films were carried out in a liquid (Hepes-NaCl buffer containing 0.15 M NaCl and 20 mM Hepes at pH 7.4) in contact mode using a Nanoscope V atomic force microscope (AFM; Veeco, California). Pyramidal silicone nitride cantilevers (MLCT-Microlever Probes, Veeco Instruments, Germany) with force constants around 60 mN m^{-1} were used. AFM imaging of photopatterned films was performed in the intermittent-contact mode with a PicoPlus microscope (Agilent Technologies) equipped with a 100-μm scanner. The analyses were realized in 0.15 M NaCl solution (pH 7.4) using the MAC mode. A type I MAC lever (Agilent Technologies) with a magnetic coating covering the backside of the cantilever was used. The resonance frequency of the cantilever was ∼45 kHz in water, and its nominal spring constant 0.11 N m^{-1}. The analysis of the images was performed using homemade procedures developed in Igor Pro (Wavemetrics, version 6.05).

Bacterial Assays. *L. lactis* NZ3900 and fluorescent *E. coli* TOP10 and MG1655 (strains kindly provided by Institute of Life Science and Institute de Duve of UCL, Belgium) were precultured overnight at 37 °C while shaking in GM17 medium (supplemented with 0.5% glucose) and Luria−Bertani (LB) broth (purchased from Sigma-Aldrich), respectively. Two 10 mL aliquots of these bacterial suspensions were centrifuged (10^3 rpm for 5 min at 4 °C) to harvest the bacterial cell pellets, which were subsequently resuspended in a 0.15 M NaCl sterile solution. The pH of the NaCl solution was fixed at 6.3 and 7 for *L. lactis* and *E. coli*, respectively. The cells were rinsed twice by centrifugation/resuspension cycles to ensure complete removal of the culture media.

The film-coated glass slides were introduced into 24-well plates and 2 mL of diluted bacteria suspension (10^7 colony forming units CFU mL^{-1} measured via optical density) was added. After 1 h at room temperature without shaking, the samples were removed from the wells, gently rinsed with 0.15 M NaCl solution to remove nonadhered bacteria, immersed in 5 mL of reconstituted chemically defined medium (CDM) supplemented with 1% glucose and M9 supplemented with 0.2% glucose, leucine and/or cassine for *L. lactis* and *E. coli*, respectively, then incubated at 30 and 37 °C under gentle shaking for *L. lactis* and *E. coli*, respectively. The pH of the medium was fixed at 6.4 and 7 (by adding 0.1 M NaOH or 0.1 M HCl) for *L. Lactis* and *E. coli*, respectively, to optimize the bacterial growth conditions.[44,45] pH measurements were regularly performed in the medium during the tests to check the stability of the growth conditions. Moreover, some assays were performed while changing the CDM medium once during the experiment to assess whether this operation affects the bacterial multiplication onto the sample surface. After a given time, the samples were removed, gently rinsed with buffer solution, and observed with an optical microscope to estimate the growth of the adhered bacteria. The experiments were performed in triplicate on three different dates for each bacterial strain.

To check that *E. coli* and *L. lactis* properly grew during the experiments, control tests were simultaneously performed in solution. For this, bacteria were suspended in CDM media with an initial concentration of 1 × 10^7 and 5 × 10^7 CFU mL^{-1} for *E. coli* and *L. lactis*, respectively, then exposed to the same experimental conditions than used for the growth of bacteria onto the film surface. The

multiplication of bacterial cells in CDM was followed by measuring the increase of the optical density of the suspension as a function of the time. The results obtained for *E. coli* and *L. lactis* are displayed in Figure S1 (Supporting Information).

The viability of bacteria adhered onto polyelectrolyte films was estimated by means of the LIVE/DEAD BacLight viability kit L7007 (Molecular Probes) containing SYTO 9 and propidium iodide dyes according to the procedure described elsewhere.[46]

Microscopy Observations. To estimate bacterial growth onto the films, first assays were performed to enumerate the colony forming units obtained after detachment of the bacteria from the film surface and their subsequent culture on agar plates. However, it was shown that the conditions used to detach bacteria from the film surfaces affect significantly their culturability. For this reason, film surfaces samples were observed after bacterial incubation with an optical inverted epifluorescence microscope (Zeiss Axio Observer A1, Germany) equipped with a CCD camera. The acquired images were analyzed with a homemade routine program working in Igor Pro Software (version 6.05, WaveMetrics, Inc.). This routine program automatically recognized the cell contour line and determine the average surface area covered by bacteria per field of view. Briefly, the initial color image was transformed in a gray image, then flattened by a Gaussian high-pass filter. Thresholding the image with a constant threshold allowed us to separate the bacteria from background. The thresholded image was used to compute statistics. At least 6 images per sample were acquired to perform statistical analysis. Experiments were performed in triplicate for each condition tested.

RESULTS AND DISCUSSION

Film Characterization. To assess the influence of the LbL film stiffness on bacterial behavior, non-cross-linked and photo-cross-linked (PLL/HAVB$_{37}$) films were prepared. UV−vis spectroscopy measurements performed on these films clearly revealed the disappearance of the absorbance peak centered at 252 nm after UV exposure (Figure 1). This feature testifies of the complete conversion of benzyl groups grafted onto the HA chains and, consequently, of the formation of carbon−carbon cross-links inside the films as discussed in detail in our previous study.[42] Note that this reaction corresponds only to the transformation of two vinyl groups (−CH═CH$_2$) into four methylene groups (−CH$_2$−). Accordingly, the comparison of FTIR spectra measured on the same films before and after UV-cross-linking revealed that the chemistry of the films remained essentially unchanged upon UV irradiation (Figure 1).

To assess whether the photo-cross-linking reaction affects the surface morphology of the films, AFM imaging was performed in liquid on both non-cross-linked and photo-cross-linked (PLL/HAVB$_{37}$)$_{12}$ multilayers (Figure 2). Topographical images did not show a significant variation of morphology between both samples. The roughness (root-mean-squared (rms)) computed from these AFM images showed only minor variations from 6.3 ± 1.3 nm to 4.7 ± 2.3 nm for non-cross-linked and photo-cross-linked films, respectively.

Contact angle measurements performed in the captive air bubble configuration with the sample immersed in Milli-Q water, revealed that the cross-linking process did not affect the wettability of the film surface since a contact angle of 24 ± 5° was measured for both non-cross-linked and photo-cross-linked films (Figure S2).

AFM nanoindentation measurements performed previously by our groups on (PLL/HAVB$_{37}$)$_{12}$ hydrated films prepared in the same conditions showed that the elastic modulus varies from 30 to 150 kPa for non-cross-linked and cross-linked multilayers, respectively.[42,43]

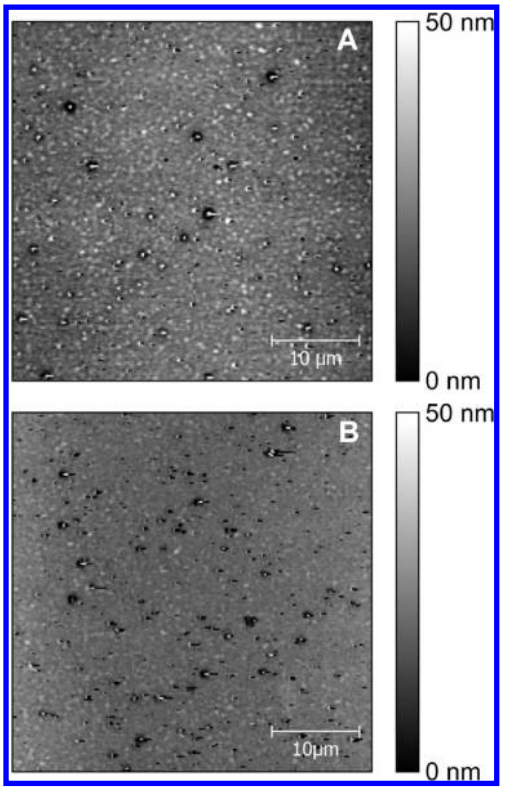

Figure 2. AFM topography images of non-cross-linked (A) and photo-cross-linked (B) hydrated (PLL/HAVB$_{37}$)$_{12}$ films.

Altogether, these results show that photo-cross-linkable (PLL/HAVB$_{37}$) multilayers are of interest to investigate the influence of substrate stiffness on cell behavior since the chemistry and morphology of these films remain essentially unchanged after photo-cross-linking while their elastic modulus increases.[42,43]

Another advantage of the (PLL/HAVB$_{37}$) system is the possibility to prepare patterned films showing a pattern of rigidity through a photolithography process. Such patterned films offer the possibility to investigate simultaneously the behavior of cells on both stiff and soft regions. To perform such a study, we prepared photopatterned films according to the process described in Scheme 2. A representative AFM phase image of a photopatterned film composed of 5 × 5 μm^2 stiffer cross-linked features distributed in a softer non-cross-linked background is displayed in Figure 3. The pattern of rigidity is clearly visible from the phase contrast. Moreover, the photo-cross-linked features show a higher phase angle, which is in agreement with a higher rigidity.[47]

Bacterial Assays. Two types of model bacteria, Gram positive *L. lactis* and Gram negative *E. coli*, were tested for their adhesive properties on these films to investigate the bacterial response versus both film stiffness and cell-type. Two strains of *E. coli*, namely, MG1655, which is widely used as a model *E. coli* K-12 wild-type, and TOP 10, which is directly derived from MG1655, were tested to investigate whether small genetic variations influence the bacterial behavior onto the surfaces. Image processing was performed on microscopy images to measure the average surface area covered by bacteria per field of view (Figure 4).

The results obtained were computed as the percentage of surface coverage. Observations performed on the samples after 1 h of immersion into bacterial suspensions revealed that

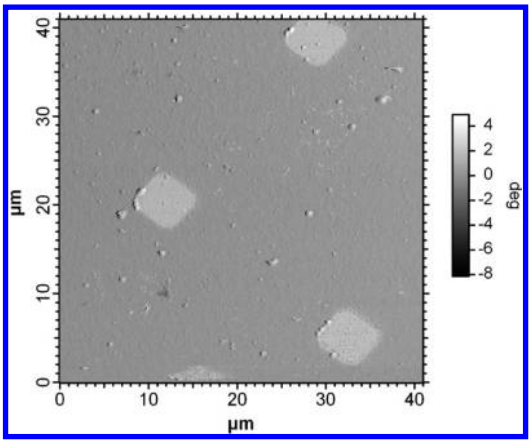

Figure 3. AFM phase image of photopatterned $(PLL/HA\text{-}VB)_{12}$ film fabricated by photolithography. The lighter zones correspond to photo-cross-linked regions of higher stiffness.

adhered microorganisms covered less than 4% of the film surface (Table 1). These results are consistent with the weak adhesive properties of highly hydrophilic films incorporating HA toward bacteria.[6,48] Interestingly, the surface coverage was slightly higher of about 17−31% on stiffer cross-linked films compared to the softer non-cross-linked ones independently of the bacterial type. These results are in agreement with previous results obtained by Van Vliet et al.,[34] who showed that the stiffer films facilitated the initial adhesion of bacteria, as usually observed for eukaryotic cells. The limited difference of elastic modulus of about 120 kPa measured by AFM nanoindentations between stiffer photo-cross-linked and softer non-cross-linked $(PLL/HAVB_{37})$ films[42,43] may explain the relative small difference in bacterial adhesion observed between both films. Moreover, viability tests performed by means of the Live/Dead BacLight kit revealed that the adherent bacteria were essentially viable as attested by their green staining (Figure 5; results shown only for *L. lactis*).

Following the adhesion tests, growth experiments were performed with both bacterial strains in CDM. The relative bacterial growth on the films was estimated by computing the relative variation of the covered surface according to the following equation:

$$\text{Relative growth} = [(\text{covered surface})_t - (\text{covered surface})_0] / (\text{covered surface})_0 \quad (1)$$

with t corresponding to the time of growth. Beyond a short latency period of about 2 h, which certainly resulted from the stress suffered by bacteria during medium change between the adhesion tests and the growth experiments, the growth of bacterial microcolonies was observed on films for both *L. lactis* and *E. coli* strains. Moreover, viability tests performed with the Backlight kit evidenced that the most of these adhered bacteria were alive, even after a culture time of 8 h. However, kinetics measurements based on the estimation of the film surface covered by bacteria as a function of the time revealed very different growth behaviors between *L. lactis* and *E. coli* bacteria. Gram positive *L. lactis* grew continuously and very slowly on both tested films (Figure 6). The relative growth after 8 h was only of about 35% and 60% on non-cross-linked and cross-linked films, respectively.

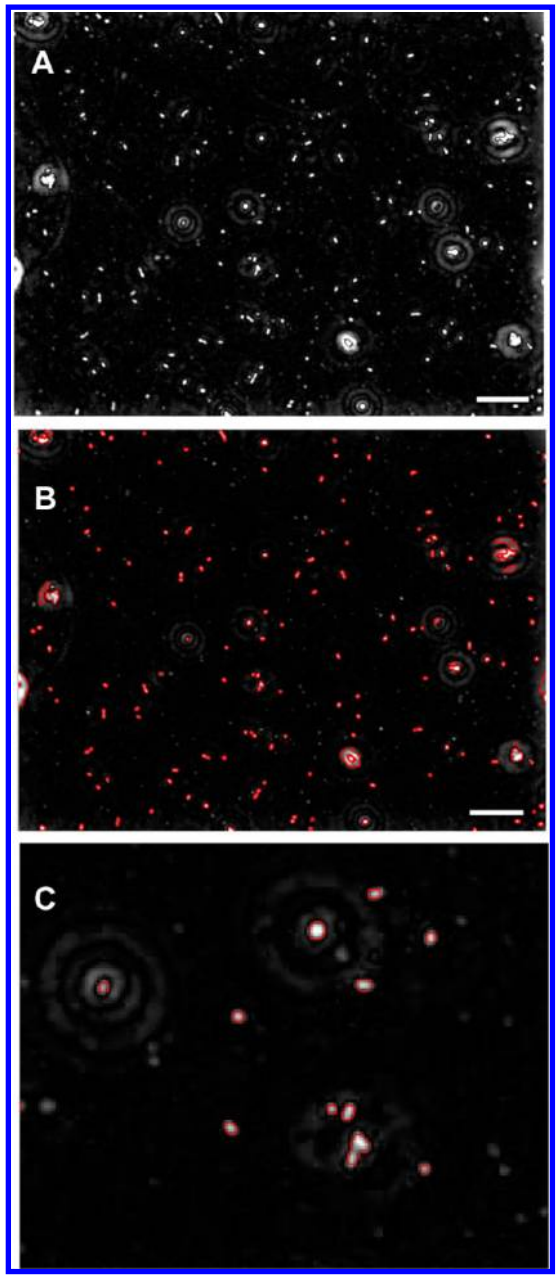

Figure 4. Determination of the surface area covered by bacteria from image analysis: (A) optical microscopy image of *L. Lactis* adhered on a $(PLL/HAVB_{37})_{12}$ polyelectrolyte film; (B) determination of the bacterial cell contour line by image processing (see Experimental Section); (C) Zoom-in image of (B). The scale bars represent 10 μm.

By contrast, the Gram negative *E. coli* showed a more complex behavior and appeared to be more affected by the film stiffness (Figure 7). On softer non-cross-linked films, the surface area covered by bacteria first increased with time to reach a maximum, then slightly decreased. Although this behavior was observed for both *E. coli* tested strains, it was more pronounced for *E. coli* M6155, which showed a much higher growth. This behavior appeared for the two strains, regardless of whether the growth medium was replaced (TOP 10) or not (M6155) during the culture. Therefore, its most likely origin is the detachment of microcolonies from the film surface as was already described in a previous report.[49] Indeed, when the size of the microlonies become large enough, they tend to detach from the surface to disseminate themselves in

Table 1. Quantification of Bacterial Adhesion onto Photo-Cross-Linked and Non-Cross-Linked Films after 1 h of Immersion in Bacterial Suspension

	Percentage of surface area covered by bacteria[a]		
	non-cross-linked films	cross-linked films	relative difference in covered surface between non-cross-linked and cross-linked films
L. lactis	1.60 ± 0.09	2.10 ± 0.09	+ 31%
E. coli TOP10	2.75 ± 0.05	3.24 ± 0.08	+ 18%
E. coli M6155	1.04 ± 0.11	1.22 ± 0.15	+ 17%

[a]All data computed expressed as ± standard deviation; each average value computed from the analysis of 15 different 111 × 85 μm^2 images recorded on 2 × 3 different samples prepared on three different dates.

the surrounding environment. On photo-cross-linked films, the growth of *E. coli* also reached a maximum after 4.5−6 h. However, for both strains, bacterial growth was much lower and much slower on these stiffer films than on non-cross-linked ones. Indeed, after 4.5 h of culture, the relative bacterial growth was of about 80 and 1600% on non-cross-linked films for *E. coli* TOP10 and *E. coli* M6155, respectively. In contrast, the relative growth on photo-cross-linked films reached a maximal value of only 20 and 545% for *E. coli* TOP10 and *E. coli* M6155, respectively. Therefore, even if M6155 strain grew more rapidly than TOP10 strain, both bacteria responded similarly to film stiffness: the lower the film stiffness, the higher and faster the cell growth.

To conclude definitely about the influence of the film stiffness on *E. coli* behavior, growth tests were performed with M6155 strain onto photopatterned films showing a micropattern of rigidity. Such experiments allowed to investigate simultaneously the behavior of cells on softer and stiffer regions. A representative image of the distribution of the cells observed after 4.5 h on photopatterned films is shown in Figure 8. Interestingly, a higher number of bacteria was observed on softer background and on the border between softer and stiffer regions. Moreover, image processing performed on 21 microscopy images recorded in three different experiments revealed that the number-average size of bacterial microcolonies is 3 ± 0.5 and 1.6 ± 0.3 μm^2 onto softer and stiffer zones, respectively, whereas the relative surface occupied by the

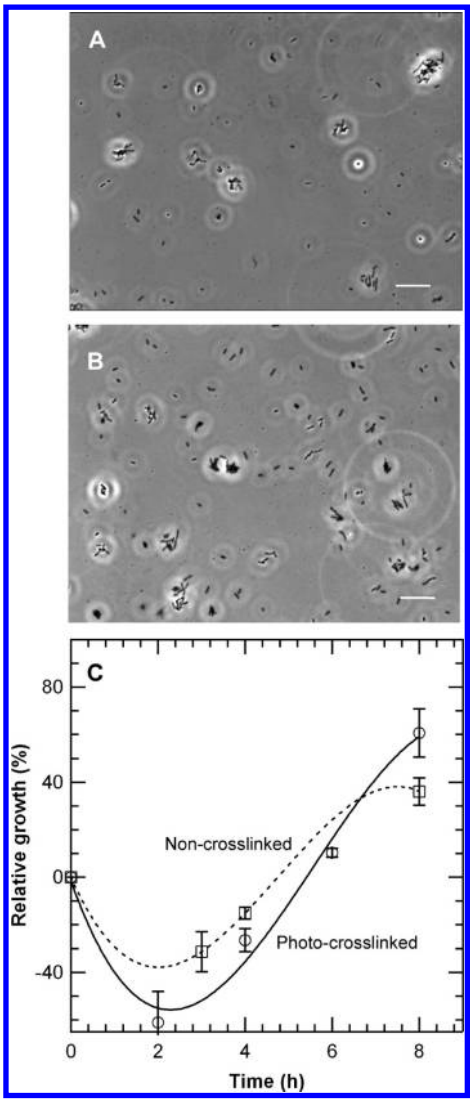

Figure 6. Optical microscopy images showing *L. lactis* after 8 h of growth on non-cross-linked (A) and photo-cross-linked films (B). Relative growth of *L. lactis* estimated from the relative variation of the covered surface on non-cross-linked (square) and cross-linked (circle) films (C). The error bars represent the standard deviation calculated from the analysis of 18 frames recorded on three different samples. The scale bars represent 10 μm.

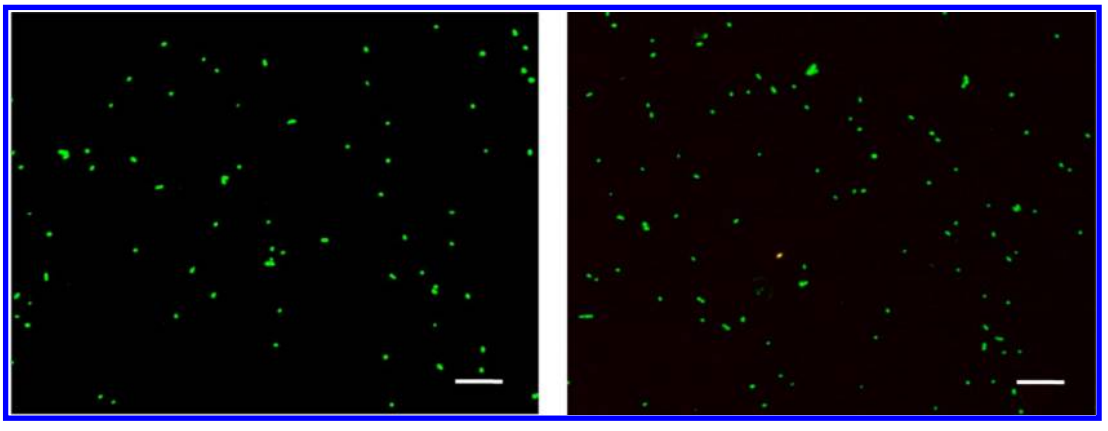

Figure 5. Fluorescence overlay microscopy images of *L. lactis* adhered onto non-cross-linked (left) and photo-cross-linked films (right) and stained with Live/Dead BacLight kit. The overlay images are built from green and red channel images. The scale bars represent 10 μm.

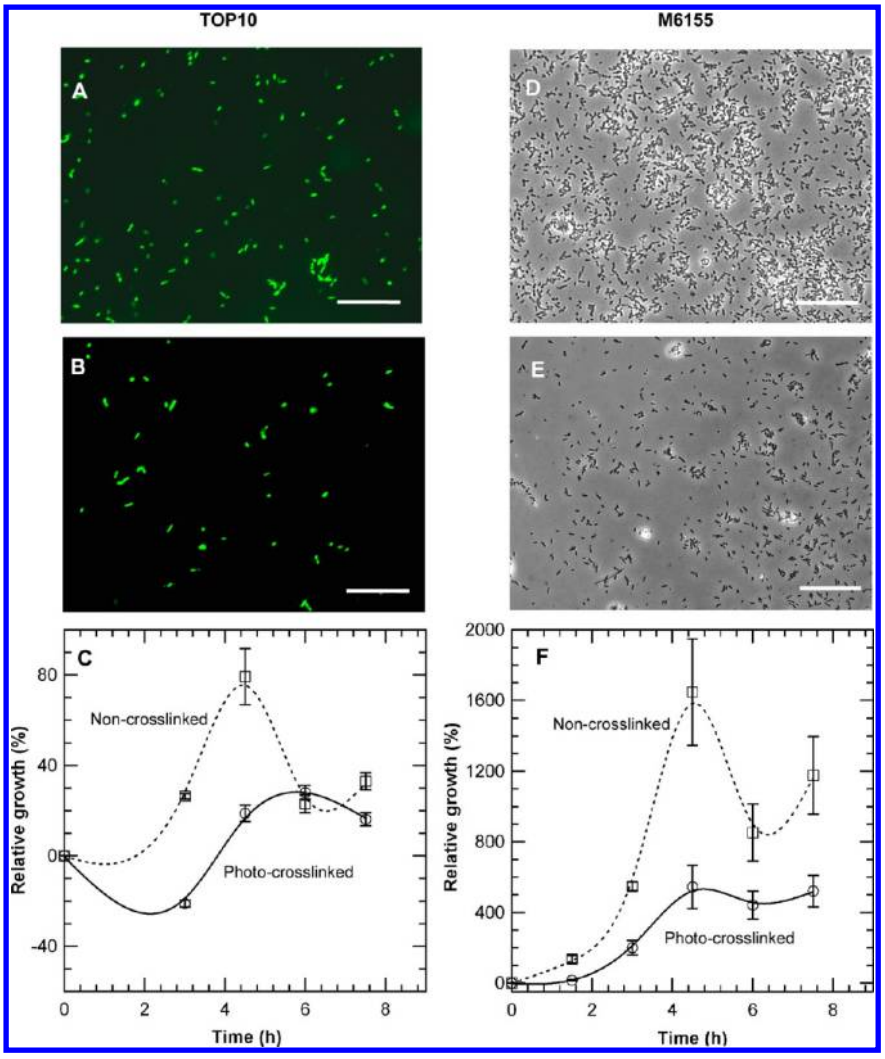

Figure 7. Microscopy images showing *E. coli* TOP 10 (left) and *E. coli* M6155 (right) after 4 h and 30 min of growth on non-cross-linked (A,D) and cross-linked films (B,E); Relative growth of *E. coli* TOP 10 (C) and *E. coli* M6155 (F) estimated from the relative variation of the covered surface on non-cross-linked (square) and photo-cross-linked (circle) films. The error bars represent the standard deviation calculated from the analysis of 18 frames recorded on three different samples prepared at different dates. The scale bars represent 10 μm.

bacteria was on average 1.75 times larger on the non-cross-linked regions compared to photo-cross-linked ones.

This result provides the evidence that *E. coli* bacteria grow more rapidly on softer films than on stiffer ones. This feature contrasted drastically with the behavior observed previously for myoblast cells, for which a higher and a faster cell proliferation rate was measured on cross-linked films.[42]

The behavior of *E. coli* contrasts also with *L. lactis*, which was shown to be not significantly affected by the film stiffness. Such a difference between both bacteria may be explained by considering the varying composition and structure of the cell wall between both bacteria. Indeed, *L. lactis* is a Gram positive and nonmotile bacteria whose wall is essentially composed of a thick layer of partially cross-linked peptidoglycan.[50] This peptidoglycan forms a rigid three-dimensional structure that certainly limits the mechanoselectivity of the cell toward the substrate. By contrast, the cell wall of the Gram negative *E. coli* is composed of a thin layer of peptidoglycan covered by lipopolysaccharides, which form a soft external layer.[50,51] Additionally, the surface of *E. coli* is decorated by various protein appendices such as flagella, pili, or fimbriae, which play a crucial role in the adhesion and motility of the cell.[51] These surface structures seemed to be more sensitive to the surface rigidity.

The fact that *E. coli* growth was higher and faster on non-cross-linked films might tentatively be explained by the fact that first adhered bacteria detached more easily from softer substrates and, then grew rapidly in solution and redeposited onto the film surface. However, since much larger colonies were observed on the softer parts of the patterned films compared to the stiffer ones, this argument does not appear likely.

The higher development of *E. coli* on softer films might also be tentatively ascribed to an easier partial reorganization of the polyelectrolyte chains in the softer films, due to the surface force exerted by bacterial cells, compared to the stiffer cross-linked films. This hypothesis should be explored in further works.

Our results contrast with the previous study reported by van der Mei et al., who reported that marine bacteria adhered in higher numbers on PU substrates of higher rigidity, in the GPa range.[35,36] Van Vliet et al.[34] also showed that the development of bacterial colonies correlated positively with an increase of the film stiffness in the 1−100 MPa range, independently of the bacterial strain. Both studies thus involved substrates of

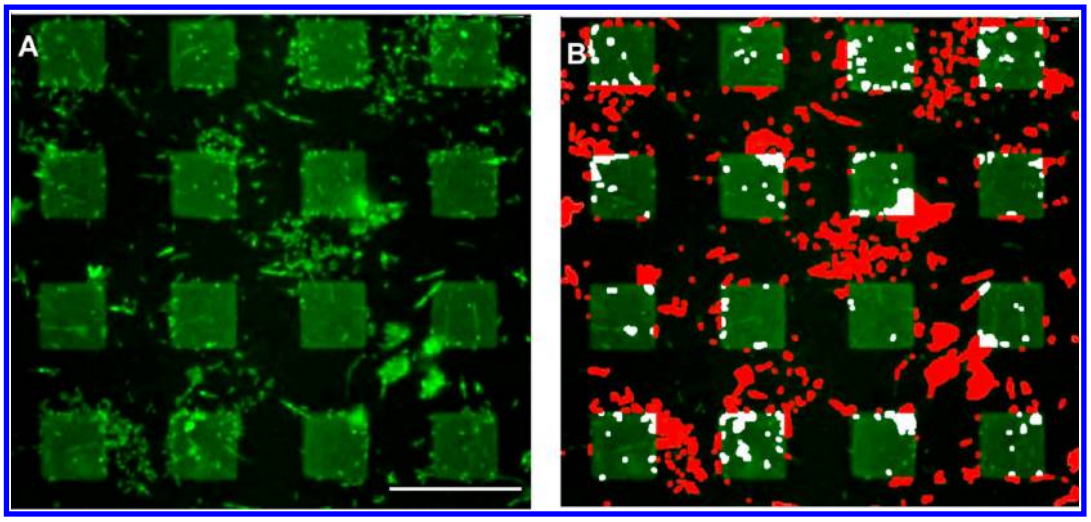

Figure 8. (A) Microscopy epifluorescence image showing *E. coli* M6155 after 4.5 of growth on photopatterned films; the lighter 20 × 20 μm^2 features correspond to stiffer photo-cross-linked regions while the dark background corresponds to the non-cross-linked film. The fluorescent contrast observed between the features and the background results from the presence of a photomask incorporated into the transparent fused silica substrate used to prepare the film. The scale bar represents 40 μm. (B) Analysis of the same image to discriminate the bacteria colonies adhered on the photo-cross-linked regions (white patches) and the non-cross-linked background (red patches). For this specific image, the relative surface occupied by the bacteria is 8 and 12% over photo-cross-linked and non-cross-linked regions.

significantly higher rigidities compared to ours (30−150 kPa), which is a first reason for the differences of behavior seen in the present work. In addition, the chemistry and morphology of our biopolymer-based films are quite different from the ones of these previous studies which were based on synthetic materials; since chemical variations are an important aspect in the bacterial response, our observations are not contradictory with these previous reports. In our study, the variation of the film stiffness was obtained via photo-cross-linking performed after film preparation, with minimal variations of film chemistry and microstructure as shown by AFM, contact angle, and spectroscopy measurements (Figures 1 and 2).[42] Therefore, the results observed here may be explained solely by the variation of film stiffness in the 30−150 kPa range.

The variability in the results obtained on different LbL systems and bacterial strains evidence that the experimental conditions used for the tests have to be taken carefully into consideration to definitely conclude about the systematic behavior of the cells. Bacterial adhesion and growth are affected by various factors including the composition of the environment, the characteristics of the bacteria itself, and the characteristics of the targeted surface. Our system offers the possibility to compare the influence of the film stiffness on the bacterial behavior, independently from the variation of the parameters cited above.

CONCLUSION

The development of biofunctional surfaces that promote the adhesion of mammalian cells while preventing bacterial colonization is a key challenge in the field of tissue engineering field. However, the fearful ability of bacteria to colonize any kind of surface makes the work highly laborious. In this context, any strategy influencing negatively bacterial growth and positively mammalian cell development is of great interest. In the present work, polyelectrolyte films whose nanomechanical properties can be varied simply under UV illumination while keeping constant the other surface characteristics were used to systematically investigate the influence of the film stiffness on the bacterial behavior. Studies performed with different types of bacteria revealed that the growth of selected Gram negative bacteria was clearly influenced by the stiffness of the coating, which was not the case for Gram positive bacteria. This feature was explained by considering the surface characteristics of both cells. More interestingly, it was shown that the growth of Gram negative bacteria was slowed down on stiffer films compared to the softer ones. This result is of particular interest since it drastically contrasts with the behavior observed previously for mammalian cells.[42] Therefore, the surface stiffness seems to be a relevant parameter that should be exploited to regulate the surface colonization by both mammalian and bacteria cells. The stiffer photo-cross-linked LbL films based on PLL and HAVB are notably interesting coatings for tissue engineering applications since they promote cell adhesion while limiting bacterial proliferation.

ASSOCIATED CONTENT

Supporting Information

Figures showing the growth of *L. lactis* at 30°C and *E. coli* M6155 at 37°C followed in CDM and a typical image of a captive air bubble deposited onto a photo-cross-linked $(PLL/HAVB_{37})_{12}$ film in water. This material is available free of charge via the Internet at http://pubs.acs.org.

AUTHOR INFORMATION

Corresponding Author

*E-mail: karine.glinel@uclouvain.be; phone: ++32 10 47 35 58; fax: ++32 10 45 15 93.

Notes

The authors declare no competing financial interest.

ACKNOWLEDGMENTS

We thank Prof. A. M. Jonas (UCL) for the image analysis routine program, S. Derclaye and Dr. C. Marie (UCL) for their technical assistance with the bacterial assays, Prof. B. Nysten for technical assistance with AFM, Prof. P. Soumillon, Prof. J.-F. Collet, and Prof. P. Hols (UCL) for kindly providing the

bacterial strains, and Prof. Y. Dufrêne (UCL) for helpful discussions. Dr. T. Boudou is thanked for his assistance with AFM measurements. K.G. benefits from a "M.I.S - Mandat ULYSSE" from the Belgium F.R.S. FNRS. This research is performed within the frame of the International Doctoral School in Functional Materials funded by the ERASMUS MUNDUS Programme of the European Union and within the frame of the French-Belgium Tournesol Programme (Project 26595ZJ). C.P. wishes to thank the European Research Council for financial support (ERC Starting Grant GA 259370).

REFERENCES

(1) Habash, M.; Reid, G. *J. Clin. Pharmacol.* **1999**, *39*, 887−898.
(2) Costerton, J. W.; Stewart, P. S.; Greenberg, E. P. *Science* **1999**, *284*, 1318−1322.
(3) Costerton, B.; Cook, G.; Shirtliff, M.; Stoodley, P.; Pasmore, M. Biofilms, Biomaterials and Device-Related Infections. In *Biomaterials Science: An Introduction to Materials in Medicine*, 2nd ed.; Ratner, B. D., Hoffman, A. S., Schoen, F. J., Lemons, J. E., Eds.; Elsevier Academic Press: San Diego, CA, 2004; pp 345−354.
(4) Gottenbos, B.; Busscher, A. J.; Van der Mei, H. C.; Nieuwenhuis, P. *J. Mater. Sci.: Mater. Med.* **2002**, *13*, 717−722.
(5) Subbiahdoss, G.; Kuijer, R.; Busscher, H. J.; van der Mei, H. C. *Microbiology* **2010**, *156*, 3073−3078.
(6) Chua, P. H.; Neoh, K. G.; Kang, E. T.; Wang, W. *Biomaterials* **2008**, *29*, 1412−1421.
(7) Tiller, J. C.; Liao, C. J.; Lewis, K.; Klibanov, A. M. *Proc. Natl. Acad. Sci. U.S.A.* **2001**, *98*, 5981−5985.
(8) Lawson, M. C.; Shoemaker, R.; Hoth, K. B.; Bowman, C. N.; Anseth, K. S. *Biomacromolecules* **2009**, *10*, 2221−2234.
(9) Kohnen, W.; Kolbenschlag, C.; Teske-Keiser, S.; Jansen, B. *Biomaterials* **2003**, *24*, 4865−4869.
(10) Lichter, J. A; Van Vliet, K. J.; Rubner, M. F. *Macromolecules* **2009**, *42*, 8573−8586.
(11) Klibanov, A. M. *J. Mater. Chem.* **2007**, *17*, 2479−2482.
(12) Livermore, D. *Rev. Microbiol.* **2004**, *2*, 73−78.
(13) AshaRani, P. V.; Low Kah Mun, G.; Hande, M. P.; Valiyaveettil, S. *ACS Nano* **2009**, *3*, 279−290.
(14) Liu, J.; Hurt, R. H. *Environ. Sci. Technol.* **2010**, *44*, 2169−2175.
(15) Ploux, L.; Ponche, A.; Anselme, K. *J. Adhes. Sci. Technol.* **2010**, *24*, 2165−2201.
(16) An, Y. H.; Friedman, R. J. *J. Biomed. Mater. Res.* **1998**, *43*, 338−348.
(17) Katsikogianni, M.; Missirlis, Y. F. *Eur. Cells Mater.* **2004**, *8*, 37−57.
(18) *Handbook of Bacterial Adhesion: Principles, Methods, and Applications*; An, Y. H., Friedman, R. J., Eds.; Humana Press: Totowa, NJ, 2000.
(19) Anselme, K.; Davidson, P.; Popa, A. M.; Giazzon, M.; Liley, M.; Ploux, L. *Acta. Biomater.* **2010**, *6*, 3824−3846.
(20) Hochbaum, A. I.; Aizenberg, J. *Nano Lett.* **2010**, *10*, 3717−3721.
(21) Singh, A. V.; Vyas, V.; Patil, R.; Sharma1, V.; Scopelliti, P. E.; et al. *PLoS One* **2011**, *6*, e25029.
(22) Puckett, S. D.; Taylor, E.; Raimondo, T.; Webster, T. J. *Biomaterials* **2010**, *31*, 706−713.
(23) Diaz, C.; Cortizo, M. C.; Schilardi, P. L.; Gomez de Saravia, S. G.; Fernandez Lorenzo de Mele, M. *Mater. Res.* **2007**, *10*, 11−14.
(24) Rizzello, L.; Sorce, B.; Sabella, S.; Vecchio, G.; Galeone, A.; Brunetti, V.; Cingolani, R.; Pompa, P. P. *ACS Nano* **2011**, *5*, 1865−1876.
(25) Discher, D. E.; Janmey, P.; Wang, Y.-L. *Science* **2005**, *310*, 1139.
(26) Ito, Y. *Soft Matter* **2008**, *4*, 46−56.
(27) Anselme, K.; Ploux, L.; Ponche, A. *J. Adhes. Sci. Technol.* **2010**, *24*, 831−852.
(28) Pelham, R. J.; Wang, Y. L. *Proc. Natl. Acad. Sci. U.S.A.* **1997**, *94*, 13661−13665.
(29) Richert, L.; Boulmedais, F.; Lavalle, P.; Mutterer, J.; Ferreux, E.; Decher, G.; Schaaf, P.; Voegel, J.-C.; Picart, C. *Biomacromolecules* **2004**, *5*, 284−294.
(30) Richert, L.; Schneider, A.; Vautier, D.; Vodouhe, C.; Jessel, N.; Payan, E.; Schaaf, P.; Voegel, J.-C.; Picart, C. *Cell Biochem. Biophys.* **2006**, *44*, 273−285.
(31) Discher, D. E.; Mooney, D. J.; Zandstra, P. W. *Science* **2009**, *324*, 1673−1677.
(32) Saha, K.; Keung, A. J.; Irwin, E. F.; Li, Y.; Little, L.; et al. *Biophys. J.* **2008**, *95*, 4426−4438.
(33) Tse, J. R.; Engler, A. J. *PLos One* **2011**, *6*, e15978.
(34) Lichter, J. A.; Thompson, M. T.; Delgadillo, M.; Nishikawa, T.; Rubner, M. F.; Van Vliet, K. J. *Biomacromolecules* **2008**, *9*, 1571−1578.
(35) Bakker, D. P.; Busscher, H. J.; van Zanten, J.; de Vries, J.; Klinjnstra, J. W.; van der Mei, H. C. *Microbiology* **2004**, *150*, 1779−1784.
(36) Bakker, D. P.; Huijs, F. M.; de Vries, J.; Klinjnstra, J. W.; Busscher, H. J.; van der Mei, H. C. *Colloids. Surf. B* **2003**, *32*, 179−190.
(37) Decher, G. *Science* **1997**, *277*, 1232−1237.
(38) Hammond, P. T. *Curr. Opin. Colloid Interface Sci.* **2000**, *4*, 430−442.
(39) Boudou, T.; Crouzier, T.; Ren, K.; Blin, G.; Picart, C. *Adv. Mater.* **2010**, *22*, 441−467.
(40) Picart, C. *Curr. Med. Chem.* **2008**, *15*, 685−697.
(41) Schneider, A.; Francius, G.; Obeid, R.; Schwinté, P.; Hemmerlé, J.; Frisch, B.; Schaaf, P.; Voegel, J.-C.; Senger, B.; Picart, C. *Langmuir* **2006**, *22*, 1193.
(42) Pózos Vázquez, C.; Boudou, T.; Dulong, V.; Nicolas, C.; Picart, C.; Glinel, K. *Langmuir* **2009**, *25*, 3556−3563.
(43) Monge, C.; Saha, N.; Boudou, T.; Pózos-Vásquez, C.; Dulong, V.; Glinel, K.; Picart, C. *Adv. Funct. Mater* **2013**, in press.
(44) Deghorain, M.; Fontaine, L.; David, B.; Mainardi, J.-L.; Courtin, P.; Daniel, R.; Errington, J.; Sorokin, A.; Bolotin, A.; Chapot-Chartier, M.-P.; Hallet, B.; Hols, P. *J. Biol. Chem.* **2010**, *285*, 24003−24013.
(45) Reshes, G.; Vanounou, S.; Fishov, I.; Feingold, M. *Phys. Biol.* **2008**, *5*, 46001.
(46) Laloyaux, X.; Fautré, E.; Blin, T.; Purohit, V.; Leprince, J.; Jouenne, T.; Jonas, A. M.; Glinel, K. *Adv. Mater.* **2010**, *22*, 5024−5028.
(47) Magonov, S. N.; Elings, V.; Whangbo, M. H. *Surf. Sci.* **1997**, *375*, L385−L391.
(48) Richert, L.; Lavalle, P.; Payan, E.; Shu, X. Z.; Prestwich, G. D.; Stoltz, J.-F.; Schaaf, P.; Voegel, J.-C.; Picart, C. *Langmuir* **2004**, *20*, 448−458.
(49) Ploux, L.; Beckendorff, S.; Nardin, M.; Neunlist, S. *Colloids Surf. B* **2007**, *57*, 174−181.
(50) Silhavy, T. J.; Kahne, D.; Walker, S. *Cold Spring Harbor Perspect. Biol.* **2010**, *2*, a000414.
(51) Ruiz, N.; Kahne, D.; Silhavy, T. J. *Nature* **2006**, *4*, 57−66.